PHYSICAL REVIEW B VOLUME 16, NUMBER 3 1 AUGUST 1977

Ballistic phonons and the transition to second sound in dilute mixtures of ^{3}He in liquid ^{4}He

R. B. Kummer, V. Narayanamurti, and R. C. Dynes
Bell Laboratories, Murray Hill, New Jersey 07974
(Received 28 December 1976)

Using the fast-heat-pulse technique we have studied the transition from ballistic phonon propagation to second sound in dilute mixtures of ^{3}He in liquid ^{4}He. At low temperatures and pressures the phonons are scattered primarily by the ^{3}He quasiparticles. Phonon-quasiparticle scattering times were determined by analyzing the pulse shapes in the transition region. These scattering times were found to be in reasonably good agreement with those theoretically calculated for Rayleigh-like scattering by Baym and Ebner, although the temperature dependence of our data was somewhat weaker than the T^{-4} behavior predicted by the theory. Our data are also in good agreement with the effective scattering times inferred from recent thermal conductivity measurements in mixtures by Rosenbaum *et al.* The phonon-quasiparticle scattering times were found to increase significantly with increasing pressure in qualitative agreement with both the theory and the thermal conductivity results. The velocity of second sound in the mixtures was measured and compared with calculated velocity curves assuming various models for the excitation spectrum. It was shown that using the Landau-Pomeranchuck spectrum for the ^{3}He quasiparticles and the normal ^{4}He excitation spectrum leads to a velocity curve which, while in qualitative agreement with the experimental data, falls somewhat below the data at $T \gtrsim 0.7$ K. The so-called "^{3}He roton" model yields a velocity curve which is in even *greater* disagreement with the experimental results. These measurements suggest the necessity for more detailed theoretical work on the elementary excitation interactions in mixtures, particularly in the region near the ^{4}He roton minimum.

I. INTRODUCTION

Heat-pulse techniques have been used extensively in the past to study second sound in liquid He II.[1] The velocities of heat pulses above about 0.7 K have been accurately determined and agree extremely well with second-sound velocities obtained from continuous-wave measurements. At lower temperatures, however, the phonon mean free path becomes quite long, and most of the earlier measurements were limited either by the use of long narrow tubes where wall collisions were important, or by the use of carbon heaters and bolometers with slow thermal response times. Under these conditions most of the heat pulses observed at low temperatures had a shape characteristic of diffusion. The wall scattering problem was essentially eliminated in the work of Gurnsey and Luszczynski[2] who, however, still had to use rather wide pulse widths because of the continued use of carbon heaters and bolometers.

Experiments have recently been performed using extremely fast metallic thin-film heaters and highly sensitive superconducting bolometers.[3] These permitted the use of much narrower pulse widths and shorter propagation lengths than had been used previously. By studying the transition from "ballistic" phonon flow at low temperatures to second sound at higher temperatures, a great deal of information was obtained about the lifetimes and scattering mechanisms of the elementary excitations—phonons and rotons—in the liquid. The fast-heat-pulse technique has similarly been used to study elementary excitations and second sound in other systems, including solid ^{3}He and ^{4}He.[4]

In the present work, this method is applied to dilute mixtures of ^{3}He in liquid ^{4}He. Measurements were made in the temperature range 0.05–1.5 K with ^{3}He concentrations [$X = n_3/(n_3+n_4)$, where n_3 and n_4 are the numbers of moles of ^{3}He and ^{4}He, respectively] from less than 10^{-3} up to about 10^{-2}. At three concentrations data were taken at pressures of 5, 15, and 24 bar as well as at the saturated vapor pressure (SVP). Excellent (quasi-) ballistic[5] phonon pulses were observed at the lowest temperatures in each case. The transition from ballistic phonon flow to second sound in the elementary excitation "gas" (consisting of ^{3}He quasiparticles, phonons, and, at higher temperatures, rotons) was investigated. Within a certain range of concentrations, temperatures, and pressures, it was possible to determine phonon-^{3}He quasiparticle scattering rates from an analysis of the phonon pulse shapes. These scattering rates are compared with those inferred from recent thermal conductivity measurements[6] as well as with the theoretical calculations of Baym and Ebner.[7]

The data presented here represent, as far as we know, the first observation of ballistic phonons in ^{3}He-^{4}He mixtures. While in previous heat-pulse experiments in mixtures[8,9] diffusive phonon signals were, in some cases, observed,[9] the phonon-quasiparticle scattering rates (or scattering lengths) derived from these data must be regarded as pre-

liminary in view of the strong dependence of the pulse shape on input heat-pulse energy in this region. This point will be discussed more fully in Sec. III.

The second-sound velocities measured in this experiment are compared with calculated values using various models for the excitation spectrum in mixtures. The temperature interval 0.7–1.5 K is particularly interesting because the calculated second-sound velocities in this region are sensitive to the excitation spectrum at intermediate momenta—a region which has recently generated a great deal of controversy.[10–13] The compatibility of the various models with these data and with the results of other experiments relating to the excitation spectrum in mixtures is discussed.

II. EXPERIMENTAL TECHNIQUES

Most of the experimental apparatus and techniques used in this work have been described elsewhere.[3] We discuss in this section only the salient features particular to this experiment.

The heat-pulse generator was a Constantan film heater ~500 Å thick with a resistance of ~50 Ω. The detector was an indium film bolometer with a thickness of ~1500 Å. The thermal response times of such devices have been found to be less than 10^{-8} sec.[14] The bolometer was biased with a constant dc current of ~400 μA and then magnetically tuned to near the midpoint of its resistive transition for maximum sensitivity. Both the heater and bolometer were ~3.5×3.5 mm^2. The pulse progagation length was 2.60 mm. This value was determined by accurately measuring the time delay between peaks of successive echoes of the second-sound signal in pure ^{4}He at the temperature ($T \approx 1.1$ K) of the well-known velocity minimum.[1]

Heat pulses were generated by an HP 214A pulse generator. The amplitude of the voltage pulse used throughout most of this experiment was 1.0 V yielding a heater power per unit area of ~1.6 mW/mm^2. Pulse widths were typically 0.2–1.0 μsec. Voltage pulses from the bolometer were amplified and recorded by a Biomation 8100 transient recorder and were then signal averaged by a Nicolet model 1074 signal averager. In the case of the weakest signals (in the ballistic–second-sound transition region) over 16 000 individual pulses were averaged. Typical pulse repetition rates were 20–80 sec^{-1}.

Temperatures above 0.2 K were measured with a commercially calibrated four-terminal germanium resistance thermometer (Scientific Instruments, Inc., Lake Worth, Fla.). At lower temperatures a carbon resistance thermometer, which had been previously calibrated against a cerium-magnesium-nitrate (CMN) thermometer, was used. The magnetoresistance of the germanium thermometer in the small fields used to bias the bolometer (~500 G) was measured and found to introduce less than a 3-mK error in temperature above 0.2 K. Our overall uncertainty in temperature is estimated to be about 10 mK below 0.5 K and 2% at higher temperatures.

The ^{3}He-^{4}He mixtures used in the present experiment were purchased with specified ^{3}He molar concentrations from Mound Laboratory, Miamisburg, Ohio. In some cases pure ^{4}He was added to the mixtures in gaseous form at room temperature, and the concentrations were recomputed based on the known amounts of gas involved. A mass spectroscopic analysis of two of the samples was made at the end of the experiment and showed that the computed concentrations were accurate within the experimental uncertainty of 10%.

Steps were taken to minimize the decrease in ^{3}He concentration of the liquid in the cell due to the enriched concentration in the vapor above the liquid.[15] A small-diameter (0.35-mm) sample-cell fill line, which was valved off at the top of the cryostat, was used to minimize the volume of vapor. For each sample the cell was initially filled at a temperature less than 200 mK by allowing the premixed sample gas to condense in from a room-temperature storage tank, and the fill-line valve was closed immediately after the cell was completely filled with liquid. Upon completing the SVP data, the remaining sample gas was pumped from the storage tank using a charcoal-filled cryopump, and the cell was pressurized by warming the cryopump above 4.2 K. The data were always taken at successively increasing pressures in order to avoid drawing off any enriched vapor.

III. BALLISTIC AND TRANSITION REGIONS

A. Qualitative features

Typical pulse shapes at several temperatures at SVP and at 24.0 bar are shown in Figs. 1 and 2, respectively. The transition from ballistic phonon flow to second sound may be clearly seen in these figures. Before discussing the data in detail, we will give a brief qualitative discussion of some of the physical mechanisms which determine the pulse shapes at low temperatures.

In general, a heat pulse produces a cloud of phonons at the surface of the heater. In the absence of scattering, these phonons travel ballistically to the detector producing a well-defined pulse. The sharp leading edge of this pulse arrives with a transit time corresponding to the velocity of sound (~238 m/sec for ^{4}He at SVP). The exact shape of the pulse, including the position of the peak, is influenced by geometrical factors and, particularly

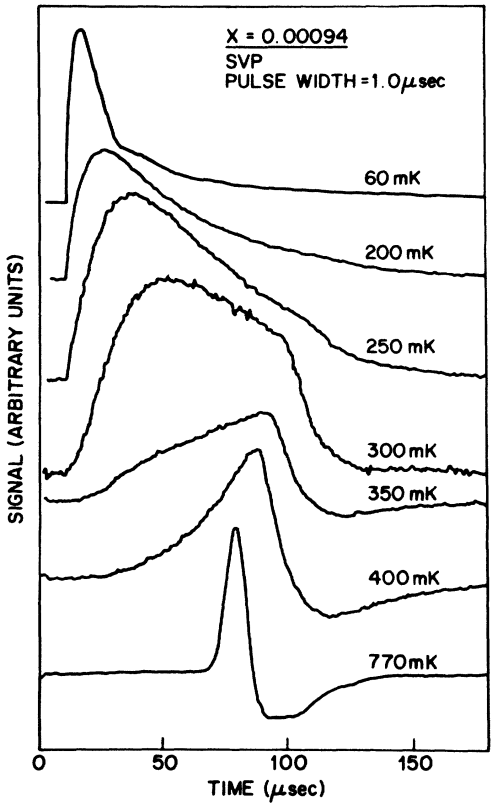

FIG. 1. Pulse shapes at SVP showing the transiton from essentially ballistic phonon propagation to second sound. ^{3}He concentration $X = 0.00094$. Cell length = 2.60 mm. The 1.0-μsec input pulse width is five times larger than that used at low temperatures for the pulses which were analyzed quantitatively.

at very low temperatures, by the power and width of the heat pulse. The distribution of phonon velocities is determined by the phonon frequency spectrum which, in turn, depends on the heater surface temperature. In the limit of very low heater power, i.e., where the heater surface temperature during a pulse is only infinitesimally greater than the bulk liquid temperature T, the dominant phonon frequency is expected to be given approximately by $\omega_d = 3.8\, k_B T/\hbar$. Larger heater powers produce more high-frequency lower-velocity phonons, thus broadening the pulse and retarding the peak. Furthermore, large pulse powers and pulse widths can increase the temperature of a certain volume of liquid near the heater to a value well above the ambient temperature, possibly to a temperature region where appreciable scattering occurs within the heated volume. As the phonon cloud travels through the liquid, the energy within the heated volume is dissipated radially and the effective "temperature" of the pulse (as determined by the amount of scattering) approaches the ambient value. This effect again tends to broaden the pulse and results in a dependence of peak velocity on cell length. Thus the importance of using small heater powers and pulse widths in obtaining power-independent data is clear.

At this point we should discuss the significance of the quantity which we call "peak heat-pulse velocity"—i.e., the propagation length divided by the arrival time of the pulse peak. Within the framework of the present method of analysis (see Sec. III B) the pulse is treated as a "half-cycle" of a continuous wave. The arrival time, in this model, is analogous to a "phase shift" in a cw experiment. Thus we treat the peak pulse velocity as a "phase velocity," although, strictly speaking, phase velocity is only well defined for a continuous wave.

It should be emphasized that, in the dispersive region where the mean free path is of the order of the cell length, the peak velocity is strongly dependent on cell length (even in the absence of the heating effects discussed above) since changing the cell length is equivalent to measuring the velocity at a

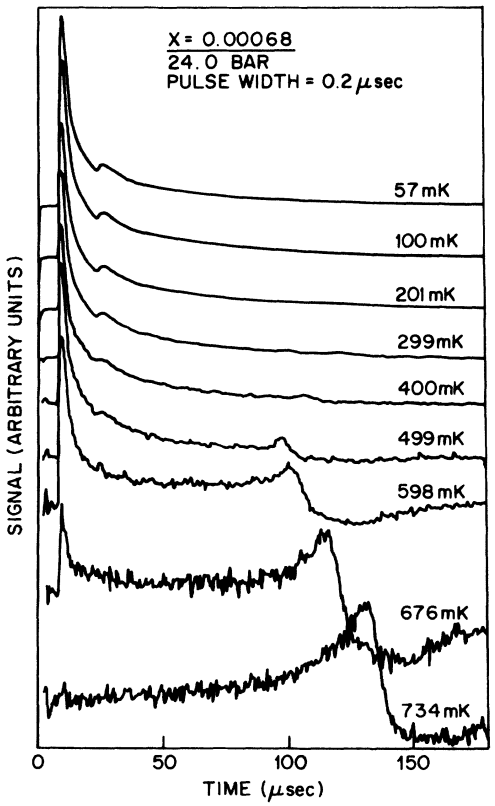

FIG. 2. Typical pulse shapes at 24.0 bar showing reduced phonon scattering at high pressures. Ballistic "echo" signal clearly evident up to $T \approx 500$ mK. $X = 0.00068$; cell length = 2.60 mm; input pulse width = 0.2 μsec.

different wave vector k. This does not affect the final results for the scattering time, however, because the effective pulse "frequency" [see Eq. (2), Sec. III B] also changes in a compensating manner.

Considering now the SVP data shown in Fig. 1, we observe an essentially ballistic pulse at the lowest temperature (60 mK). Following the initial pulse there is evidence of a weak phonon "echo" pulse arriving at approximately three times the transit time of the main pulse. As the temperature is increased, phonon scattering begins to occur, and the pulse is broadened and eventually begins to take on a diffusive-like shape. Since (large-angle) phonon-phonon and phonon-roton scattering are known to be quite weak at these temperatures,[3,5] the dominant scattering mechanism in this region is phonon-^{3}He quasiparticle (p-qp) scattering.

At temperatures near 250–300 mK, p-qp scattering is sufficiently strong that a collective second-sound mode begins to develop in the phonon-quasiparticle gas. By ~400 mK the second-sound mode is fully developed, and there is no longer any evidence of a ballistic or diffusive phonon signal.

The effect of pressure on the pulse shapes is seen in Fig. 2. The striking feature of these data, taken at a pressure of 24.0 bar, is that the ballistic pulse retains its narrow width at temperatures up to about 700 mK, indicating that the p-qp scattering times are larger (or at least not significantly smaller) than the pulse propagation time (~10 μsec) even at this relatively high temperature. A well-defined phonon echo signal is observed up to about 400 mK. The second-sound mode begins to form around 400–500 mK. Since the heater cannot excite ^{3}He quasiparticles directly, the second-sound mode is presumably excited, in this case, by roton-quasiparticle scattering (rotons begin to be thermally populated in appreciable numbers in this temperature region) and possibly by weak residual scattering of higher-frequency phonons as well.

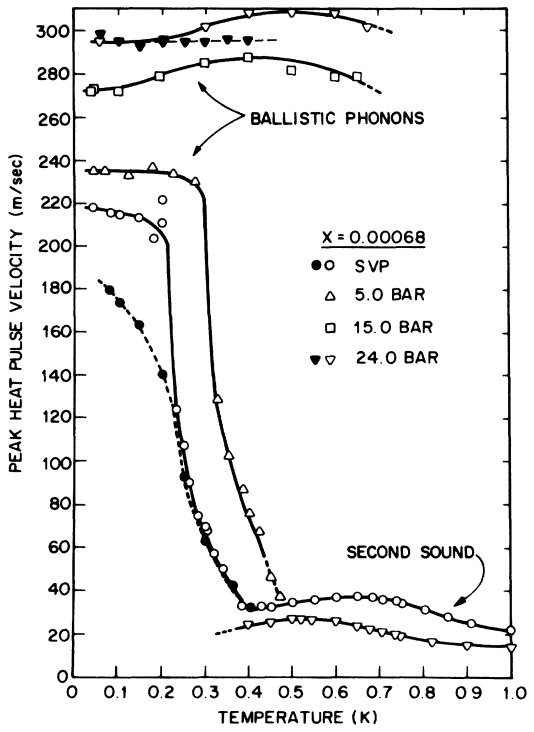

FIG. 3. Peak heat-pulse velocity versus temperature at four pressures for $X = 0.00068$. In the second-sound region only data at two pressures are shown for clarity. Effects of input pulse width are also shown: pulse width, 0.2 μsec (open symbols), 0.8 μsec (closed symbols).

In Fig. 3 we have plotted the peak heat-pulse velocity versus temperature for a given concentration at four pressures. (We emphasize that the values plotted represent the velocity of the heat-pulse peak, which, as discussed previously, may be dependent upon input pulse energy as well as the length of the sample cell; the leading edge of the phonon pulse, however, is always at the sound velocity.) The reduced phonon scattering at higher pressures is evidenced in the figure by the increased temperature region over which the ballistic velocity is approximately constant. The figure also illustrates the effect of input heat-pulse width on the received pulse shape. The SVP data with an input pulse width of 0.8 μsec (closed symbols) never reach a ballistic "plateau" and fall considerably below the 0.2-μsec data (open symbols) at temperatures less than about 0.25 K. At higher temperatures the two sets of data are in good agreement, indicating that we are measuring approximately ambient-temperature excitations in this region. At temperatures less than ~0.15–0.20 K, however, even the 0.2-μsec data probably do not represent ambient thermal excitations, since a further reduction in pulse energy in this region results in a further increase in peak pulse velocity. For this reason only data taken at $T \gtrsim 0.2$ K were used in the quantitative pulse-shape analysis to be discussed in Sec. III B.

The slight increase in ballistic pulse velocity near 0.5 K seen at the two highest pressures is only slightly greater than the experimental scatter in the data, but seems to occur consistently at all concentrations. If we assume that this is a real effect, it probably results from a weak scattering of high-frequency lower-velocity phonons out of the pulse. As we will discuss in Sec. III B, p-qp scattering is expected to be a Rayleigh-like process with an ω^4 frequency dependence.

The effect of ^{3}He concentration on the pulse velocity is shown in Fig. 4. It is interesting to note that the limiting low-temperature "ballistic" vel-

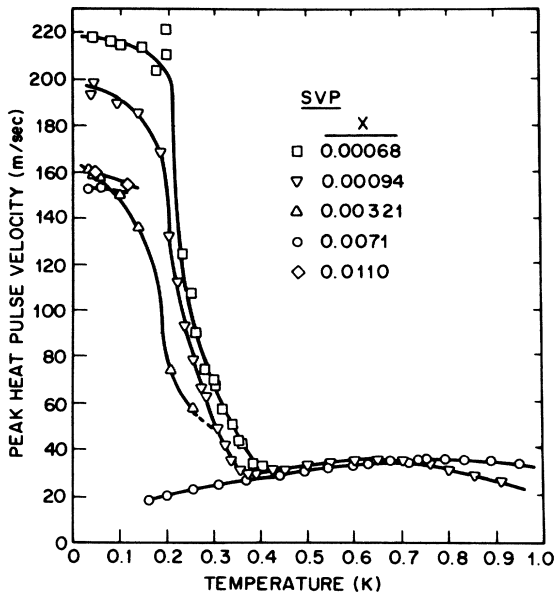

FIG. 4. Peak heat-pulse velocity vs temperature at SVP for several values of ^{3}He concentration (X). In the second-sound region only data at two concentrations are shown for clarity. Input pulse width, 0.2 μsec.

ocity seems to reach a minimum value near $X = 0.007$. As pointed out earlier, phonon scattering can occur within a small volume near the heater which may be heated above the ambient temperature. This effect almost certainly occurs in the lowest-temperature data. The amount of scattering, and hence the delay of the pulse, is influenced both by the ^{3}He concentration and the temperature to which the volume is heated. The latter decreases with increasing concentration due to the increasing heat capacity of the mixture. Thus the competing effects of these two factors could result in the observed behavior.

B. Pulse-shape analysis

The procedure used to calculate p-qp scattering times from the data has been applied previously to phonon scattering in solids[4,16] as well as in pure ^{4}He.[3] This method utilizes a general dispersion relation for temperature waves derived by Rogers.[16] Using *hydrodynamic* equations and assuming plane-wave solutions for the temperature, the heat-flow equation was solved to yield[16]

$$\tfrac{1}{3}k^2v_1^2=\omega^2+i\omega/\tau_R+i\omega k^2\tau(v_1^2-v_2^2)/(1-i\omega\tau)\,, \qquad (1)$$

where $\tau^{-1}=\tau_N^{-1}+\tau_R^{-1}$. Here v_2 is the velocity of (phonon) second sound (not the velocity of quasiparticle second sound in a mixture), and v_1 is the first-sound velocity. τ_N and τ_R are the scattering times for normal- and resistive-process scattering, respectively. k is the wave number and ω is the angular frequency of the temperature wave.

Equation (1) may be solved for the phase velocity $v=\mathrm{Re}(\omega/k)$ of the temperature wave as a function of the product $\omega\tau$. The result is plotted in Fig. 5 for $\tau_R \ll \tau_N$ (solid line) and for $\tau_R \gg \tau_N$ (dashed line) using values of v_1 and v_2 appropriate for pure ^{4}He at SVP ($v_1=\sqrt{3}v_2=238$ m/sec). For weak scattering ($\omega\tau \gg 1$), the velocity approaches the ballistic velocity v_1. In the limit of strong normal-process scattering, the velocity approaches $v_1/\sqrt{3}$, the limiting low-temperature phonon second-sound velocity in pure ^{4}He, while for strong resistive scattering the velocity continues to decrease.

It should be emphasized that Eq. (1) is derived assuming hydrodynamic behavior, and hence may not be strictly valid in the weak-scattering regime ($\omega\tau \gtrsim 1$). The limiting behavior $v \to v_1$, however, is certainly correct.

For the purposes of the present analysis, the ^{3}He quasiparticles in the mixture are treated as resistive phonon scattering centers, much like impurities or defects in a solid. This picture is probably valid in the weak and intermediate scat-

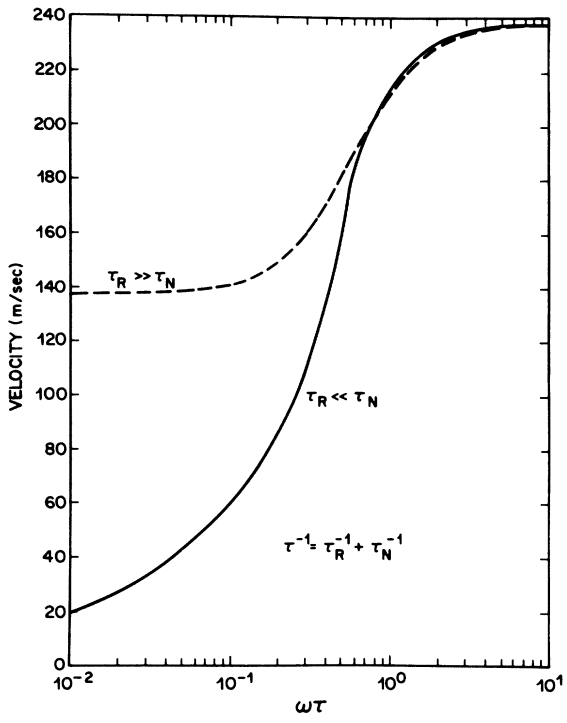

FIG. 5. Temperature wave dispersion relation, velocity [$v=\mathrm{Re}(\omega/k)$] vs $\omega\tau$, calculated from Eq. (1) with $v_1=\sqrt{3}v_2=238$ m/sec. $\tau^{-1}=\tau_R^{-1}+\tau_N^{-1}$, where τ_R and τ_N are resistive- and normal-process scattering times, respectively. Two limiting cases are shown: $\tau_R \ll \tau_N$ (solid line) and $\tau_R \gg \tau_N$ (dashed line).

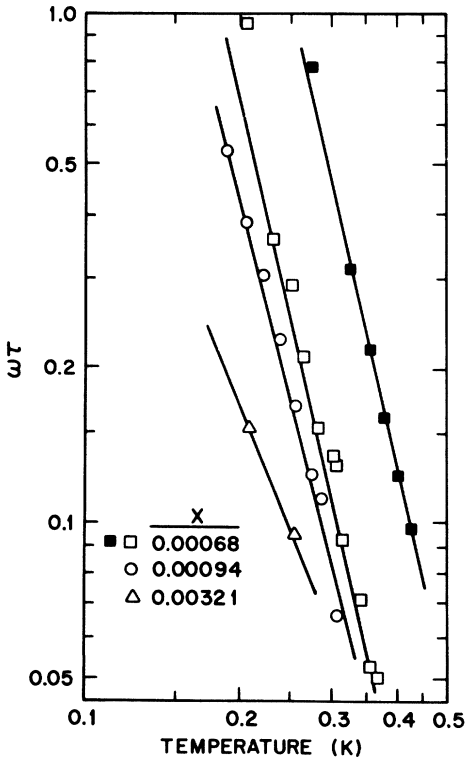

FIG. 6. $\omega\tau$ vs temperature for three concentrations at SVP (open symbols), and one at 5.0 bar (closed symbols). These $\omega\tau$ values were determined from the peak heat-pulse velocity data in the ballistic second-sound transition region (see, e.g., Fig. 4) using the dispersion relation for strong resistive scattering (the solid line in Fig. 5 for the SVP data).

tering regime ($\omega\tau \gtrsim 10^{-1}$), but not in the region of very strong scattering ($\omega\tau \lesssim 10^{-2}$) where heat propagates as a collective mode (second sound) in the entire gas of phonon, quasiparticle, and (at higher temperatures) roton excitations.

The quantities $\omega\tau$ were determined from the peak heat-pulse velocity data in the ballistic-to-second-sound transition region using the solid curve (resistive scattering) of Fig. 5 (and similar curves at pressures other than SVP). The results are shown in Fig. 6. Only data in the range $1.0 \gtrsim \omega\tau \gtrsim 0.05$ were analyzed in order to be in a region where Eq. (1) is expected to be valid as discussed above and where boundary scattering effects are unimportant (in the near-ballistic region the effective τ merely reflects the cell length). Furthermore, only data at $T \gtrsim 0.2$ K were considered since points at lower temperatures are not believed to represent ambient-temperature excitations. These restrictions were satisfied only at the three lowest concentrations at SVP and at the single lowest concentration at 5.0 bar. At higher concentrations, the second-sound mode already dominated (and the phonon signal had disappeared) at $T \approx 0.2$ K, and at higher pressures, the ballistic signal never experienced sufficient scattering for $\omega\tau \lesssim 1.0$.

It is desirable, obviously, to extract the p-qp scattering time τ from the data of Fig. 6, and this requires a knowledge of the effective "frequency" characterizing the heat pulse. The quantity ω as it appears in Eq. (1) is, strictly speaking, the frequency of a propagating temperature wave. Physically, $2\pi/2\omega$ represents the time interval during which the interaction is "active" (the factor 2 in the denominator arises from the fact that the "interaction time" is a half-cycle). For a heat-pulse experiment in the true hydrodynamic limit the interaction time is the input pulse width. In the weak-scattering regime considered in the present experiment, however, the appropriate interaction time is approximately given by the pulse propagation time t. Thus the effective pulse "frequency" is defined to be

$$\bar{\omega} \equiv 2\pi/2t = \pi d/v\,, \tag{2}$$

where d is the cell length, and v is the measured peak pulse velocity.

The effective p-qp scattering time τ was determined by dividing each $\omega\tau$ value by the corresponding effective frequency $\bar{\omega}$. The results for the two lowest concentrations at SVP are shown as open symbols in Fig. 7 where we have plotted τ multiplied by the ^{3}He concentration X (as discussed in Sec. III C, τ is expected to be inversely proportional to X) versus temperature.

C. Comparison with theory and with other experiments

In this section we compare our results with the theory of p-qp interactions in dilute mixtures developed by Baym and Ebner[7] and with the scattering times inferred from recent thermal conductivity measurements.[6] According to the Baym and Ebner theory, there are two processes which limit the phonon mean free path in mixtures at low temperatures: (i) Rayleigh-like scattering of phonons by ^{3}He quasiparticles, and (ii) absorption of phonons by ^{3}He quasiparticles, which is kinematically possible because of quasiparticle interactions.

The scattering rate for the first process has the characteristic ω^4 dependence on phonon frequency. Within the dominant phonon approximation ($\omega_d \approx 3.8\, k_B T/\hbar$) the scattering rate at SVP is given by[7]

$$\tau_{sc}^{-1} \approx 4.8\times 10^{10} X T^4 \text{ sec}^{-1}\text{K}^{-4}. \tag{3}$$

For the range of concentrations and temperatures considered here, the absorption rate varies as $\tau_a^{-1} \propto X^2 T^2$, and, as pointed out by Rosenbaum *et al.*,[6] is expected to be much smaller than τ_{sc}^{-1}. (The absorption process is expected to dominate,

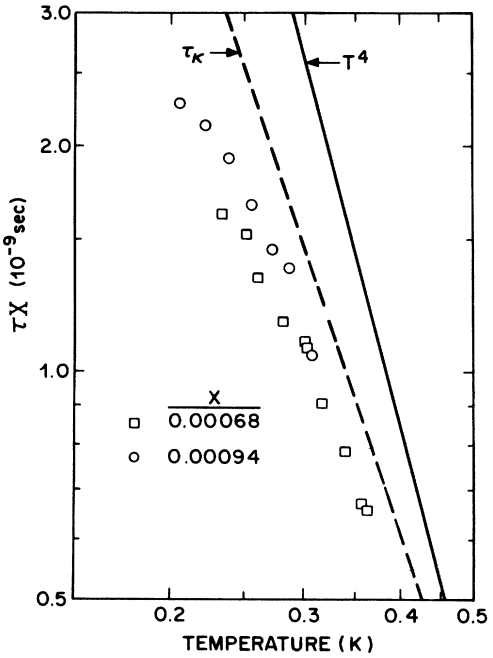

FIG. 7. Phonon-quasiparticle scattering time (τ) multiplied by ^{3}He concentration (X) vs temperature for data at the two lowest concentrations at SVP. The open symbols were obtained by dividing the corresponding $\omega\tau$ values of Fig. 6 by the effective pulse frequency $\bar{\omega}=\pi d/v$ (see text). The dashed line labeled "τ_κ" represents a least-squares fit to the effective scattering time obtained from the thermal conductivity measurements of Rosenbaum *et al.* (Ref. 6) using Eq. (4). The solid line labeled "T^4" is from the theoretical calculation of the Rayleigh-like scattering time by Baym and Ebner (Ref. 7) [Eq. (3)].

however, at very low temperatures and/or at higher concentrations.)

The quantity $\tau_{sc}X$ calculated from Eq. (3) is shown in Fig. 7 as a solid line labeled T^4. From the figure it may be seen that our data fall slightly below the theoretical curve and show a somewhat weaker temperature dependence. In view of the fact that there are no adjustable parameters in the theory, however, the overall numerical agreement with our data is considered good.

Our results may also be compared with those of recent thermal conductivity measurements in dilute mixtures by Rosenbaum *et al.*[6] In the range of temperatures and concentrations considered here, heat is transported primarily by phonons. Thus the thermal conductivity may be written

$$\kappa=\tfrac{1}{3}C_v v_1^2\tau_p, \tag{4}$$

where C_v is the phonon specific heat (i.e., the specific heat of pure ^{4}He), and v_1 is the phonon velocity (sound velocity). The total phonon scattering rate τ_p^{-1} in this region is equal to the effective p-qp scattering rate τ_κ^{-1} plus the boundary scattering rate τ_b^{-1}, which may be determined from measurements in pure ^{4}He.[17]

Equation (4) was used to calculate the effective p-qp scattering time τ_κ from the thermal conductivity data. The dashed line in Fig. 7 represents a least-squares fit to $\tau_\kappa X$ obtained in this manner from the thermal conductivity data at two concentrations ($X=0.00071$ and $X=0.00122$) in the temperature range 0.2–0.45 K. The agreement with our data, as shown in the figure, is reasonably good.

While no quantitative values are given for τ_{sc} at elevated pressures, the Baym and Ebner theory[7] does predict an increase of the scattering time with pressure. As we have pointed out earlier such an effect was observed in the present experiment. At 5.0 bar and $X=0.00068$ (the only data for which a quantitative analysis was possible) we find that τ is ~60% larger than at SVP. Using the Baym and Ebner theory, Rosenbaum *et al.*[6] estimate that τ_{sc} should be ~14 times larger at 24.0 bar than at SVP. Such a value is consistent with our failure to observe any p-qp scattering below 0.7 K at 24.0 bar (see Fig. 3).

D. Conclusions

These data, we feel, provide strong evidence for Rayleigh-like scattering of phonons by ^{3}He quasiparticles in dilute mixtures as suggested by the Baym and Ebner theory.[7] The slight numerical disagreement between our data and the theory, particularly at the lower temperatures, could conceivably result from a slight amount of excessive heating of the pulses above the ambient temperature, or from some of the assumptions involved in the analysis. The analysis is felt to be most valid at higher temperatures where the scattering is relatively strong, and thus the fact that the overall experimental temperature dependence of the scattering time seems to be weaker than predicted by the theory is not regarded as serious. Considering the simplicity of the analysis, the numerical agreement of our data with the theory, as well as with the thermal conductivity results, is quite good.

IV. SECOND-SOUND REGION

A. Excitation spectrum in mixtures

A secondary motivation for the present experiment stems from the recent controversy regarding the nature of the ^{3}He quasiparticle excitation spectrum in mixtures. The second-sound velocity curve in mixtures (below ~1.5 K) can be calculated from the excitation spectrum. Thus it was felt that an accurate measurement of the second-sound

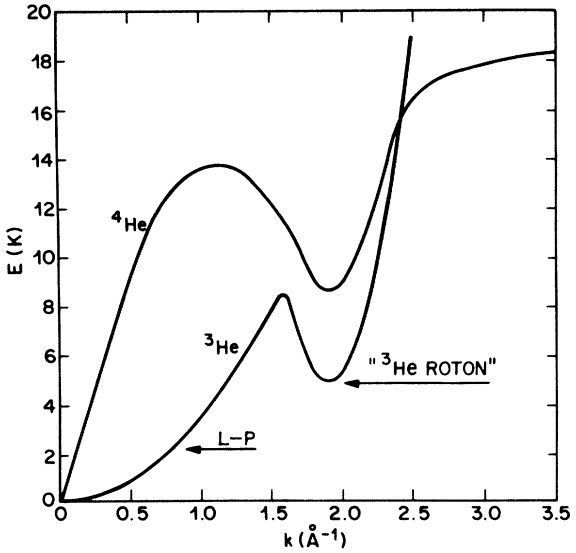

FIG. 8. "^{3}He-roton" model for the elementary excitation spectrum, E vs k, in mixtures. At $k \lesssim 1.5$ Å the ^{3}He quasiparticles are described by the Landau-Pomeranchuck spectrum of Eq. (5) with $m_3^* \approx 2.3\, m_3$. The proposed "^{3}He-roton" region [Eq. (6)] is shown at higher wave numbers. The ^{3}He roton parameters for the curve shown are $\Delta_3 = 5.0K$, $k_3 = 1.9$ Å^{-1}, and $\mu_3 = 0.2\, m_3$. The well-known ^{4}He excitation spectrum is from neutron scattering measurements at $T \approx 1.1$ K.

velocity as a function of temperature, concentration, and pressure could yield valuable information about the excitation spectrum. Before discussing our results, we will briefly review some of the theories and experiments relating to the excitation spectrum in mixtures.

The familiar ^{4}He excitation spectrum is shown in Fig. 8 with its linear phonon region at low wave numbers (k) and roton region at $k \sim 1.9$ Å^{-1}. It was proposed a number of years ago by Landau and Pomeranchuck[18] (LP) that ^{3}He atoms in solution with ^{4}He would behave as a dilute Fermi gas of quasiparticles with an excitation spectrum of the form

$$\epsilon(k) = \epsilon_0 + \hbar^2 k^2 / 2m_3^*, \tag{5}$$

where ϵ_0 is a constant, and m_3^* is an effective quasiparticle mass subsequently shown to be approximately 2.3 times the bare ^{3}He atomic mass m_3.

This model has proven quite successful in describing a large number of experiments which probe the small-k region of the excitation spectrum. Recently, however, questions have arisen regarding the shape of the excitation spectrum at k values near the ^{4}He roton minimum. Experiments involving fourth-sound propagation,[19] ion mobilities,[20] and normal-fluid density[21] in mixtures all seem to infer a significant decrease in the energy of the ^{4}He roton minimum Δ_4 with increasing ^{3}He concentration. Specifically, these experiments indicate that Δ_4 drops from its value of ~8.6 K at $X = 0$ and apparently levels off at ~5 K for $X \gtrsim 0.2$. Raman-scattering experiments,[22] which directly measure the energy of the two-roton state, on the other hand, show no significant change of Δ_4 in mixtures with X as large as 0.31.

This apparent contradiction led Pitaeveskii[10] to suggest the existence of a rotonlike region in the ^{3}He quasiparticle excitation spectrum (see Fig. 8) of the form

$$\epsilon(k) = \Delta_3 + \hbar^2 (k - k_3)^2 / 2\mu_3, \tag{6}$$

where μ_3 is an effective mass parameter, and k_3 is near the value k_0 of the ^{4}He roton minimum. The ^{3}He roton energy minimum Δ_3 would be smaller than Δ_4—presumably about 5 K. Theoretical arguments have been presented by Varma[11] and by Stephen and Mittag[12] indicating that such a ^{3}He roton branch should indeed exist. Slinkman and Ruvalds,[13] on the other hand, argue that a proper analysis of the experimental data shows that the original LP spectrum actually provides the best fit.

B. Calculation of the second-sound velocity

In view of this controversy we have investigated the nature of the excitation spectrum in mixtures through its influence on the second-sound velocity. Given the excitation spectrum and assuming strong scattering among all the excitations of the system, the Boltzmann equation may be solved for the second-sound velocity in a manner analogous to that suggested by Kwok[23] for the case of solids and used by Narayanamurti *et al.*[3] for the case of pure ^{4}He. The resulting expression for the second-sound velocity in mixtures is

$$v_2^2(T) = \tfrac{1}{3}\left(\sum_i \int \omega_i(k)\, S_i^0(k,T)\, \vec{k}\cdot\vec{u}_i(k)\, k^2\, dk\right)^2 \Big/ \left(\sum_i \int S_i^0(k,T)\, \omega_i^2(k)\, k^2\, dk\right)\left(\sum_i \int S_i^0(k,T)\, k^4\, dk\right), \tag{7}$$

where i is a two-valued branch index referring, respectively, to the ^{3}He and ^{4}He branches of the excitation spectrum, and the quantities $\vec{u}_i(k) = \vec{\nabla}_k \omega_i(k)$ are the group velocities of the two branches. The $S_i^0(k,T)$ are the occupation number functions of the two branches, with $S_3^0(k,T) = f^0(k,T)[1 - f^0(k,T)]$ and $S_4^0(k,T) = N^0(k,T)[1 + N^0(k,T)]$, where $f^0(k,T)$ and $N^0(k,T)$ are the

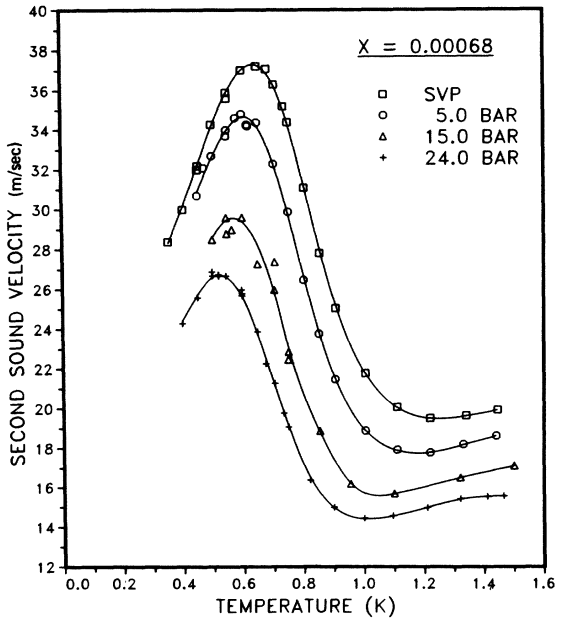

FIG. 9. Second-sound velocity versus temperature at four pressures for $X=0.00068$. The curves drawn through the data are merely to aid the eye.

equilibrium Fermi-Dirac and Bose-Einstein distribution functions, respectively. The dependence of v_2 on ^{3}He concentration X arises from the fact that the chemical potential, and hence $f^0(k,T)$, is a function of X. It should be pointed out that when calculating v_2 as a function of temperature T, the chemical potential must be recomputed at each value of T subject to the constraint that the total number of ^{3}He quasiparticles is constant.

In the case of pure ^{4}He where the only excitations at low temperatures are phonons with an excitation spectrum $\epsilon(k)\approx v_1 k$, Eq. (7) correctly leads to the limiting low-temperature second-sound velocity $v_2=v_1/\sqrt{3}$. The increasing thermal population of rotons in pure ^{4}He at temperatures above ~0.6 K results in a rapid decrease of v_2 because of the $\vec{k}\cdot\vec{u}k^2$ term in Eq. (7). As shown in Ref. 3, the experimentally measured second-sound velocity curve in pure ^{4}He below about 1.4 K agrees quite well (within a few percent) with that calculated from the ^{4}He excitation spectrum. At higher temperatures the elementary excitation picture becomes less valid as the excitations broaden considerably and become illdefined.

The addition of even a small amount of ^{3}He to ^{4}He results in a dramatic change in the velocity of second sound. At very low temperatures, Eq. (7) is dominated by the ^{3}He branch of the excitation spectrum, and for temperatures below the degeneracy temperature, the second-sound velocity approaches $v_F/\sqrt{3}$ (v_F is the Fermi velocity). In this case the second-sound mode propagates almost entirely in the ^{3}He quasiparticle gas (the quasiparticle-quasiparticle scattering times are relatively short), and cannot be excited by thermally produced phonons since the p-qp scattering times are quite long. (It can be excited, for example, by an oscillating superleak transducer as was demonstrated by Brubaker *et al.*[24] who measured the second-sound velocity in dilute mixtures down to $T\approx 0.03$ K.) As the temperature is increased the second-sound velocity increases due to the increasing velocity of the ^{3}He quasiparticles at higher k values (just as in the case of ordinary sound in a gas) and the increasing influence of the ^{4}He phonon excitation spectrum. Finally, at still higher temperatures ($T\gtrsim 0.5$ K), the ^{4}He roton branch becomes thermally populated, and the second-sound velocity eventually reaches a peak and then decreases as the influence of the rotons becomes larger.

C. Experimental results and discussion

Our experimental results for the second-sound velocity as a function of temperature at three concentrations and four pressures are shown in Figs. 9–11. The qualitative features discussed in Sec. IV B are readily seen in the data.

Our results at SVP are in excellent agreement with those of Brubaker *et al.*,[24] who measured the velocity of mechanically-induced second sound in

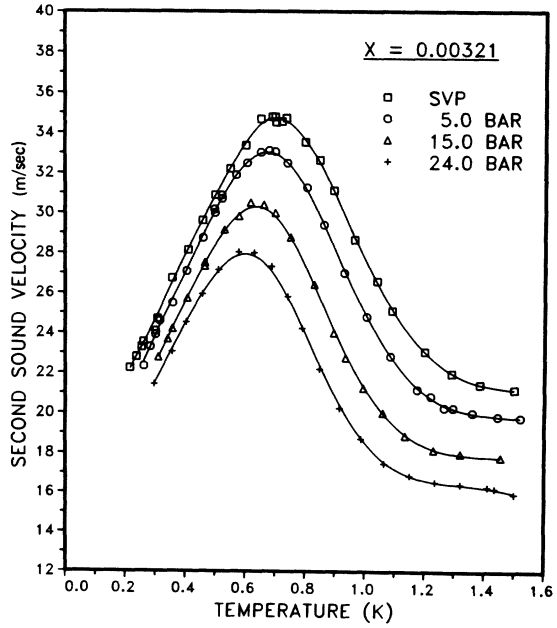

FIG. 10. Second-sound velocity versus temperature at four pressures for $X=0.00321$. The curves drawn through the data are merely to aid the eye.

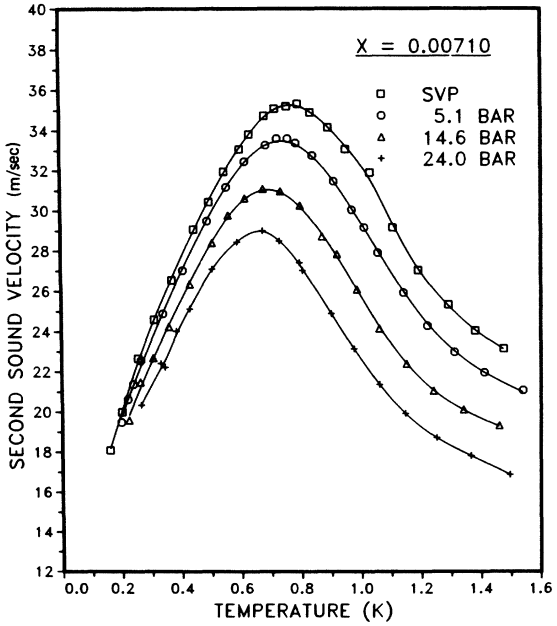

FIG. 11. Second sound velocity versus temperature at four pressures for $X = 0.00710$. The curves drawn through the data are merely to aid the eye.

dilute mixtures at temperatures below 0.6 K. At temperatures below the second-sound velocity maximum (i.e., for $T \lesssim 0.7$ K) our data are also in good agreement with those from the early heat-pulse measurements in mixtures by King and Fairbank,[8] but at higher temperatures we generally find a somewhat lower velocity than was reported by these authors. At $X = 0.0032$ (a value common to both experiments), the discrepancy is about (3–6)% in the temperature interval $0.7 \lesssim T \lesssim 1.5$ K. The experimental uncertainty of our data is believed to be (1–2)%.

Our SVP data at $X = 0.00321$ are compared in Fig. 12 with the second-sound velocity curves calculated from Eq. (7) for the same concentration. The solid curve is calculated from the LP spectrum [Eq. (5)], and the dashed curve is from the ^{3}He roton model [Eq. (6)]. (The particular ^{3}He roton parameters used are those of the excitation spectrum shown in Fig. 8.) It is clear from this figure that the LP spectrum yields a velocity curve which is in reasonably good agreement with the experimental data below about 0.7 K, but falls somewhat below the data at higher temperatures. (As in the case of pure ^{4}He, the elementary excitation picture begins to break down above about 1.4 K, and thus the calculated second-sound velocity curves are not expected to be valid in this region.) The addition of the ^{3}He roton branch to the excitation spectrum has little effect on the velocity curve below about 0.5 K as expected, but at higher temperatures makes the agreement with the experimental data even worse. Choosing different values for the ^{3}He roton parameters obviously alters the calculated second-sound velocity curve somewhat, but the result is *always* lower than that calculated with the LP spectrum which is *already* lower than the experimental data. The agreement with experiment is better at lower concentations and worse at higher concentrations, but is always qualitatively similar to that shown in Fig. 12.

From an examination of Eq. (7) it is clear that the ^{3}He roton model will yield a velocity curve which lies below that obtained from the LP spectrum, since the ^{3}He roton branch introduces lower-velocity excitations at a lower energy than a simple extension of the LP spectrum. The same is true of the addition of a term proportional to $-k^4$ to the LP spectrum, which was proposed by Brubaker *et al.*[25] to explain an apparent temperature dependence of the effective mass m_3^* obtained from second-sound measurements below 0.6 K.[26] Likewise, a reduction of the ^{4}He roton energy minimum would also lead to a decrease in the calculated second-sound velocity curve for the same reasons given above. While there is no theoretical justification for such, we have found that an *increase* of the ^{4}He roton minimum (to about 9.1 K for $X = 0.0032$) actually produces considerably better agreement with experiment for $T \gtrsim 1.0$ K, but results in a velocity maximum which is somewhat

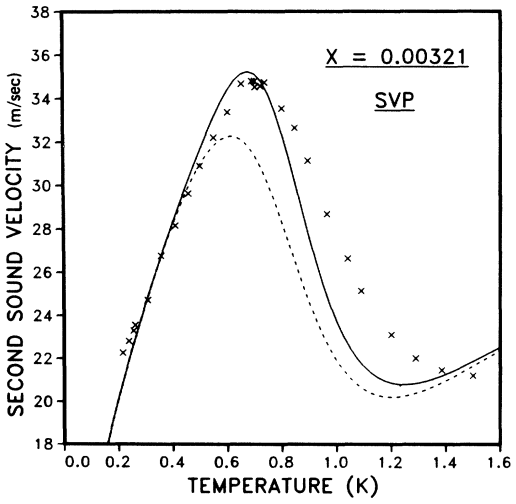

FIG. 12. Second-sound velocity vs temperature for $X = 0.00321$ at SVP. The experimental data are shown as x's. The solid and dashed curves are calculated from Eq. (7) using, respectively, the Landau-Pomeranchuck [Eq. (5)] and the "He^3-roton" [Eq. (6)] models for the He^3 quasiparticle excitation spectrum. The particular ^{3}He-roton parameters used in the latter case are those of the excitation spectrum shown in Fig. 8.

too high.

We should point out that in calculating $v_2(T)$ from Eq. (7), we have not taken into account any explicit temperature dependence of the ^{4}He excitation spectrum. As is well known, however, the excitation spectrum *decreases* slightly with increasing temperature. As we have shown, this would make the agreement with experiment even worse.

In summary, we find that the simple addition of a rotonlike branch to the ^{3}He quasiparticle excitation spectrum in mixtures is inconsistent with our second-sound velocity data. The original Landau-Pomeranchuck spectrum leads to better agreement with the experimental data than do other proposed models, but even in this case there exist significant quantitative discrepancies for $T \gtrsim 0.7$ K. While we have been unable to achieve an acceptable overall fit to the experimental data with any simple excitation spectrum model, our results seem to imply a definite shift of spectral weight in the ^{4}He roton region toward *higher* energy values.

At the high temperatures of interest ($T \gtrsim 0.7$ K) the elementary excitations in mixtures may be ill-defined due to their short lifetimes, and their interactions are probably more complicated than we have implicitly assumed in our simple calculation of the second-sound velocity. More theoretical work toward obtaining a better description of the excitations is clearly necessary.

ACKNOWLEDGMENTS

The superb technical assistance of M. A. Chin and J. P. Garno is gratefully acknowledged.

[1]See, e.g., V. P. Peshkov, Zh. Eksp. Teor. Fiz. 38, 799 (1960) [Sov. Phys.-JETP 11, 580 (1960)]; H. C. Kramers, Proc. Acad. Sci. Amsterdam B 59, 35 (1956); 59, 48 (1956).

[2]R. W. Guernsey, Jr. and K. Luszczynski, Phys. Rev. A 3, 1052 (1971).

[3]V. Narayanamurti, R. C. Dynes, and K. Andres, Phys. Rev. B 11, 2500 (1975).

[4]V. Narayanamurti and R. C. Dynes, Phys. Rev. B 12, 1731 (1975).

[5]The pulses are not truly ballistic because of the existence of small-angle three-phonon scattering which occurs in ^{4}He at low pressures due to the anomalous upward dispersion of the phonon excitation spectrum [see, e.g., R. C. Dynes and V. Narayanamurti, Phys. Rev. B 12, 1720 (1975) and references cited therein]. Since the scattering is essentially one dimensional, however, it does not significantly broaden the pulse or decrease the average phonon velocity. We will, therefore, continue to refer to such pulses as ballistic.

[6]R. L. Rosenbaum, J. Landau, and Y. Eckstein, J. Low Temp. Phys. 16, 131 (1974).

[7]G. Baym and C. Ebner, Phys. Rev. 164, 235 (1967).

[8]J. C. King and H. A. Fairbank, Phys. Rev. 93, 21 (1954).

[9]D. J. Sandiford and H. A. Fairbank, in *Proceedings of the Seventh International Conference on Low Temperature Physics* (University of Toronto Press, Toronto, 1961), p. 641; C. G. Niels-Hakkenberg, L. Meermans, and H. C. Kramers, in *Proceedings of the Eighth International Conference on Low Temperature Physics* (Butterworth, Washington, 1963), p. 45.

[10]L. Pitaeveskii, Comments at the U. S.-Soviet Symposium on Condensed Matter, Berkeley, Calif., May 1973 (unpublished).

[11]C. M. Varma, Phys. Lett. A 45, 301 (1973).

[12]M. J. Stephen and L. Mittag, Phys. Rev. Lett. 31, 923 (1973).

[13]J. Slinkman and J. Ruvalds (unpublished).

[14]R. J. von Gutfeld, A. H. Nethercott, Jr., and J. A. Armstrong, Phys. Rev. 142, 436 (1966).

[15]See, e.g., J. Wilks, *The Properties of Liquid and Solid Helium* (Clarendon, Oxford, 1967), Chap. 9.

[16]S. J. Rogers, Phys. Rev. B 3, 1440 (1971).

[17]For the data of Ref. 6, the boundary scattering was described by $\tau_b^{-1} = 1.37 \times 10^5 T^{0.25}$ sec^{-1}.

[18]L. D. Landau and I. Pomeranchuck, Dokl. Akad. Nauk. SSSR 59, 669 (1948).

[19]N. E. Dyumin, B. N. Esel'son, E. Ya. Rudavskii, and I. A. Serbin, Zh. Eksp. Teor. Fiz. 56, 747 (1969) [Sov. Phys.-JETP 29, 406 (1969)].

[20]B. N. Esel'son, Yu. Z. Kovdrya, and V. B. Shikin, Zh. Eskp. Teor. Fiz. 59, 64 (1970) [Sov. Phys.-JETP 32, 37 (1971)].

[21]V. I. Sobolev and B. N. Esel'son, Zh. Eskp. Teor. Fiz. 60, 240 (1971) [Sov. Phys.-JETP 33, 132 (1971)].

[22]C. M. Surko and R. E. Slusher, Phys. Rev. Lett. 30, 1111 (1973); R. L. Woerner, D. A. Rockwell, and T. J. Greytak, Phys. Rev. Lett. 30, 1114 (1973).

[23]P. C. Kwok, Physics (L.I. City, N.Y.) 3, 221 (1967); and C. P. Enz, Ann. Phys. (N.Y.) 46, 114 (1968).

[24]N. R. Brubaker, D. O. Edwards, R. E. Sarwinski, P. Seligmann, and R. A. Sherlock, J. Low Temp. Phys. 3, 619 (1970).

[25]N. R. Brubaker, D. O. Edwards, R. E. Sarwinski, P. Seligmann, and R. A. Sherlock, Phys. Rev. Lett. 25, 715 (1970).

[26]This temperature dependence of the effective mass is seen in our own data, and accounts for the slightly different slopes of the experimental and calculated velocity curves for temperatures below the peak when a constant m_3^* is assumed. As shown in Fig. 12, however, the deviations in this region are small compared with those at $T \gtrsim 0.8$ K.